Chinese Journal of Catalysis 64 (2024) 44–53

available at www.sciencedirect.com

ScienceDirect

journal homepage: www.sciencedirect.com/journal/chinese-journal-of-catalysis

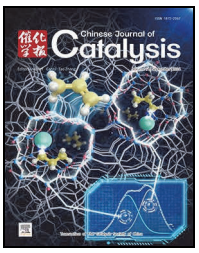

Article

# Why the abnormal phenomena of D-band center theory exist? A new BASED theory for surface catalysis and chemistry

Zelong Qiao [a], Run Jiang [a], Jimmy Yun [b,c], Dapeng Cao [a,*]

[a] *State Key Laboratory of Organic-Inorganic Composites, Beijing University of Chemical Technology, Beijing 100029, China*
[b] *Qingdao International Academician Park Research Institute, Qingdao 266000, Shandong, China*
[c] *School of Chemical Engineering, The University of New South Wales, Sydney, NSW 2052, Australia*

ARTICLE INFO

*Article history:*
Received 9 May 2024
Accepted 24 June 2024
Available online 10 September 2024

*Keywords:*
Surface chemistry
Surface catalysis
D-band center theory
Bonding orbital
Anti-bonding orbital

ABSTRACT

Since the D-band center theory was proposed, it has been widely used in the fields of surface chemistry by almost all researchers, due to its easy understanding, convenient operation and relative accuracy. However, with the continuous development of material systems and modification strategies, researchers have gradually found that D-band center theory is usually effective for large metal particle systems, but for small metal particle systems or semiconductors, such as single atom systems, the opposite conclusion to the D-band center theory is often obtained. To solve the issue above, here we propose a bonding and anti-bonding orbitals stable electron intensity difference (BASED) theory for surface chemistry. The newly-proposed BASED theory can not only successfully explain the abnormal phenomena of D-band center theory, but also exhibits a higher accuracy for prediction of adsorption energy and bond length of intermediates on active sites. Importantly, a new phenomenon of the spin transition state in the adsorption process is observed based on the BASED theory, where the active center atom usually yields an unstable high spin transition state to enhance its adsorption capability in the adsorption process of intermediates when their distance is about 2.5 Å. In short, the BASED theory can be considered as a general principle to understand catalytic mechanism of intermediates on surfaces.



## 1. Introduction

Surface chemistry is a hot topic and frontier for global researchers today, especially in electrochemistry [1–5], heterogeneous catalysis [6–10], corrosion [11–14] and other fields. How to understand the various phenomena and mechanism [15–18] of surface chemistry is the fundamental obstacle for researchers to develop new catalysts and materials. D-band center theory, which was proposed by Prof. Hammer and Prof. Nørskov *et al.* [19–23], has received widespread attention and successful application in surface chemistry field [24], where the D-band center ($\varepsilon_d$) was considered as a descriptor to predict the adsorption strength, implying that materials with low energy level of $\varepsilon_d$ would usually have weaker adsorption capability [24–26]. However, in the early time when the D-band center theory was proposed, researchers found that simple D-band center theory was insufficient to explain the adsorption behavior of very late transition metals and complex multi-metallic systems [27–29]. To solve this issue, Prof. Nørskov's group [28] further proposed a descriptor which combined the bandwidth

* Corresponding author. E-mail: caodp@mail.buct.edu.cn (D. Cao).
This work is supported by the National Key Research and Development Project (2019YFA0210300) and the National Natural Science Foundation of China (22372006).
https://doi.org/10.1016/S1872-2067(24)60100-2

of the D-band peak ($W_d$) and $\varepsilon_d$ to predict adsorption energy in 2013. On this basis, Prof. Abild-Pedersen [29] proposed the upper band edge as a key property, and further combined with $W_d$ and $\varepsilon_d$ to derive a new descriptor for better prediction in 2022. These modifications contain complex formulas and parameters, which may limit their physical meaning for investigators. Unfortunately, D-band center theory and its modifications are based on the overall properties of materials without considering adsorbates, so they have high accuracy only for the adsorption behavior of metal or alloy bulk systems with unitary active site configuration on the surface. However, for the same surfaces, different adsorption active sites [30,31] or even spin multiple states [32–34] will significantly affect the values of adsorption energy, and therefore obtain different adsorption energies. It is noted that these adsorption configurations are actually presented in experiments, and some are even the main active centers of catalysts. In this case, it is quite difficult in prediction of adsorption energies of these multiple absorbed states solely by the properties of catalytic materials without considering adsorbates.

In fact, with the increase of material types and modification methods, more and more systems yield opposite conclusions [24,35–39] with the D-band center theory, which has caused confusion for researchers. For example, for heterostructure materials with localized reactions at the interface, different intermediates may have different adsorption sites and different adsorption behavior, but the material only has one $\varepsilon_d$, while the adsorption strength of different intermediates shows an opposite trend [35,40,41]. For the clusters containing multiple index crystal surfaces, the $\varepsilon_d$ cannot accurately characterize the specific adsorption behavior of each crystal surface of clusters, which sometimes even forces researchers to calculate the ever $\varepsilon_d$ of each atom on the material [30] to obtain a more accurate prediction of adsorption energy. This implies that the advantage of the D-band center theory, which is reducing computational cost, is no longer significant. Moreover, due to the fact that the D-band center theory is based on metal bulk materials with continuous D-band [23], there is still a lack of discussion and testing on whether the newly developed single atom catalysts (SACs [38,39,42–47], which is a semiconductor catalyst and has a discontinuous D-band) can use the D-band center theory. These newly emerging materials systems often exhibit some abnormal phenomena with D-band center theory, which would lead to the confusing for researchers and therefore hinder the understanding of surface catalysis mechanism. Therefore, it is urgent to reveal the origin of the abnormal phenomena of the D-band center theory, and propose a more general theory that can predict the adsorption strength of materials based on the electronic structure.

By analyzing the fundamental origin of the abnormal phenomena of the D-band center theory, herein, we proposed a Bonding and Anti-bonding orbitals Stable Electron intensity Difference (BASED) theory, to describe interatomic interactions. The BASED can be severed as a general descriptor to accurately predict the adsorption energy ($R^2$ = 0.95) and bond length ($R^2$ = 0.94) for both SACs systems and pure metals systems. Besides, we use this descriptor to discover an interesting phenomenon, Spin Transition State (STS), during adsorption process for SACs. The STS indicates that the active center atom will open its spin and become an unstable high spin state at the distance about 2.5 Å between the active site and adsorbent, which thereby significantly improves its adsorption capability. This phenomenon provides a new physical insight for understanding the catalytic mechanisms of surface chemistry.

## 2. Density functional theory (DFT) calculation details

DFT calculations were performed through the projector augmented wave (PAW) method by using the Vienna ab initio simulation package (VASP) [48]. The Generalized gradient approximation (GGA) method with the Perdew-Burke-Ernzerhof (PBE) was adopted as the exchange-correlation functional. The k-mesh in Brillouin zones was determined based on Monkhorst-Pack kpoint grids. All the calculations use gamma-centered k-points 3×3×1, zero damping DFT-D3 method of Grimme, 500 eV cutoff energy and the spin-polarized calculations (collinear). The convergence tolerance for the residual force and energy on each atom during structure relaxation was set to 0.015 eV Å$^{-1}$ and 1 × 10$^{-5}$ eV. VASP-sol package [49] is used to simulate the solution environment for all calculations, where the dielectric constant ($\varepsilon_r$) is set to 78.5. For semiconductor systems like SACs, the Hubbard U correction (only for 3*d* TM) was also employed within the DFT+U approach, U-J: 2.11 eV for Sc, 2.58 eV for Ti, 2.72 eV for V, 2.79 eV for Cr, 3.06 eV for Mn, 3.29 eV for Fe, 3.42 eV for Co, 3.4 eV for Ni, 3.87 eV for Cu, 4.12 eV for Zn [47]. In order to accurately obtain the DOS information, we use the most precise tetrahedron method with Blöchl corrections, scatter 2000 points and completely turns off the symmetry for all electronic structure calculations to pursue sufficient accuracy. The z-direction is set to 20 Å to make the vacuum distance more than 10 Å for all the models, which is to avoid steric hindrance and interaction due to periodicity. The optimization of the unit cell parameters is carried out by the method of fixing the lattice vector, and the cell parameters are obtained as 14.903 × 12.735 × 20.000, $\alpha = \beta = \gamma$ = 90° for related calculations of SACs. And the cell parameters of the Bulks model can be obtained through separate optimization calculations: 9.370 × 10.796 × 20.000, $\alpha = \beta = \gamma$ = 90° for Pt bulk, 8.429 × 9.724 × 20.000, $\alpha = \beta = \gamma$ = 90° for Ni bulk, 9.943 × 11.399 × 20.000, $\alpha = \beta = \gamma$ = 90° for Ag bulk, 8.682 × 9.976 × 20.000, $\alpha = \beta = \gamma$ = 90° for Cu bulk. The Lobster software [50,51] performed the COHP analysis to obtain the bonding and anti-bonding information in the *d* orbital.

Calculate the adsorption energy using the following equation:

$$\Delta E_{ado^*} = E_{slab\text{-}ado^*} - E_{slab} - E_{ado^*} \quad (1)$$

where the $\Delta E_{ado^*}$ represents the adsorption energy of the active center atom on the adsorbent, $E_{slab\text{-}ado^*}$ represents the total energy of slab and adsorbent, $E_{slab}$ represents the energy of slab and $E_{ado^*}$ represents the energy of adsorbent. Notably, The structure of $E_{slab}$ needs to directly remove the adsorbent from the structure of $E_{slab\text{-}ado^*}$, and then obtain its static energy to ensure that the energy of $E_{slab}$ can represent the spin state of the active site during adsorption, which we also use in previous

work [47,52]. The adsorbents include * H, * O, * OH, and * OOH, and their corresponding energies are $E_{ado}$ shown in Table S30.

When using the BASED theory to calculate $Q$, for sites with multiple active centers (e.g., Pt/Ag/Cu/Ni Bulk), multiple bonds should be formed, so each $Q$ needs to be stacked and summed, as follows:

$$Q_{SUM} = \sqrt{{Q_1}^2 + {Q_2}^2 + {Q_3}^2 + \cdots} \quad (2)$$

The detailed $Q_{SUM}$ data obtained from this formula is shown in Tables S2–S13.

## 3. Results and discussion

### 3.1. The origin of abnormal phenomena of D-band center theory

The abnormal phenomena of D-band center theory refer to the fact that the materials with high/low energy level of $\varepsilon_d$ have weaker/stronger adsorption capability, which was also implied by Prof. Nørskov *et al*., i.e., the small metal particles have a discontinuous D-band, which could lead to the failure of the D band center theory (In Chapter 8.2 in Ref. [23]). For convenience, we marked abnormal phenomena of D-band center theory as anti-D-band center phenomenon. Obviously, if we want to reveal the intrinsic mechanism of anti-D-band center phenomenon, we need to revisit the formula of $\varepsilon_d$, given by

$$\varepsilon_d = \frac{\int_{-\infty}^{\infty} \varepsilon\rho(\varepsilon)\mathrm{d}\varepsilon}{\int_{-\infty}^{\infty} \rho(\varepsilon)\mathrm{d}\varepsilon} \quad (3)$$

where $\varepsilon$ represents the energy level, $\rho(\varepsilon)$ represents density of state (DOS) distribution. It is noted that the integration range of $\varepsilon$ is from ∞ to −∞, so the range of $\varepsilon_d$ can be higher or lower than the Fermi level. Essentially, this formula mainly calculates the energy level of the *d* orbitals for metal by using the weighted average method, with the distribution of DOS as the weight. Obviously, it seriously ignores the contribution of the electron number involved in the bonding, because it only considers the energy level. The importance of electron number for predicting adsorption energy was also mentioned in 2017 [53]. Moreover, D-band center theory only simply considers the DOS of pristine slab, so that it ignores some critical factors which significantly affect the bonding information and bonding orbitals DOS distribution during the adsorption process, e.g. magnetic moment [34,38,54–57] or internal strain [26,58,59]. Therefore, the key to reveal the intrinsic mechanism of anti-D-band center phenomenon is how to accurately depict the bonding behavior of metal active centers with adsorption intermediates.

According to modern molecular orbital (MO) theory, in the bonding process of atoms, their orbitals linearly combine to form molecular orbitals, including bonding and anti-bonding molecular orbitals. Electrons are filled in the molecular orbitals in order of energy levels from low to high. The orbitals with electron filling are called as the occupied orbitals, while the orbitals without electron filling are called as the unoccupied orbitals (empty orbitals). In general, the bonding orbital electrons could enhance the bond strength, while the anti-bonding orbital electrons would weaken the bond strength. The unoccupied orbitals have no contribution to the bond strength.

Fig. 1(a) shows that when $\varepsilon_d$ is below the Fermi level, the shift of $\varepsilon_d$ towards the lower-energy level (left shift) will lead to an increase in the proportion of anti-bonding orbitals, thereby reducing the adsorption capability of the active center. However, on the contrary, for these cases that energy level of $\varepsilon_d$ is above the Fermi level (Fig. 1(b)), the shift of the $\varepsilon_d$ towards the lower-energy level causes the proportion increase of the bonding orbitals, which enhances the adsorption capability of the active center, and thus resulting in the anti-D-band center phenomenon. Therefore, we propose that D-band center theory is valid only when $\varepsilon_d$ of pristine slab models and all the bonding orbitals of adsorption models both are completely below the Fermi level (Fig. 1(a)). Otherwise, anti-D-band phenomenon occurs when the $\varepsilon_d$ is greater than 0 eV or some bonding orbitals above the Fermi level (Fig. 1(b)), which has been observed in many works [25,37–39, 52,60].

Based on this analysis, we believe that the energy levels of both bonding and anti-bonding orbital electrons have crucial impact on adsorption energy, which is also consistent with previous research [37–39,47], i.e., the energy level difference between the occupied orbitals of the $\alpha$ and $\beta$ spin states of the adsorbed active site can serve as a descriptor to correlate adsorption energy. However, this method only considers the energy level information of α and β electron orbitals, without considering the energy levels of bonding orbitals and anti-bonding orbitals. As a result, it lacks corresponding physical insight and has a low degree of accuracy.

### 3.2. Integral crystal orbital hamiltonian population (ICOHP)

Alternatively, in 2011, Deringer *et al*. [61] improved the crystal orbital hamiltonian population (COHP) theory by using the pane wave basis sets to obtain bonding information. And in 2016, the COHP can be provided by quantum chemical programming software [50], where the negative values of COHP represent bonding orbitals, and the positive values represent anti-bonding orbitals. The integral COHP (ICOHP) has been successfully used as a descriptor to quantify the adsorption intensity [47,62] by directly integrating the COHP proportion of bonding orbitals ($\rho_{COHP\text{-}bond}$) and anti-bonding orbitals

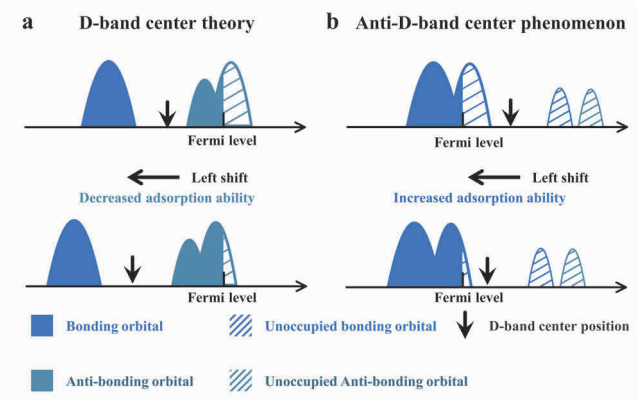


**Fig. 1.** Illustrations of D-band center theory and anti-D-band center phenomenon. (a) D-band center theory; (b) Anti-D-band center phenomenon.

($\rho_{\text{COHP-antibond}}$) to obtain the corresponding relative energy of bond strength, the unit is eV. ICOHP is usually positively correlated with the number of electrons, given by

$$ICOHP = \int_{-\infty}^{0} \rho_{\text{COHP}}(\varepsilon)d\varepsilon = \int_{-\infty}^{0} \rho_{\text{COHP-bond}}(\varepsilon)d\varepsilon - \int_{-\infty}^{0} -\rho_{\text{COHP-antibond}}(\varepsilon)d\varepsilon$$
$$= \alpha(eN_{\text{bond electrons}} - eN_{\text{anti-bond electrons}}) = \alpha eN_{\text{effective electrons}} \quad (4)$$

where $N_{\text{bond electron}}$ and $N_{\text{anti-bond electron}}$ represent the relative number of bonding and anti-bonding orbital electrons, respectively. The $e$ represents the relative energy of the electron. The $\alpha$ is the conversion coefficient between the relative energy of bond strength and the energy of electrons, which is an unitless constant. The $\varepsilon$ represents the energy level of the orbital electrons calculated by COHP method. Notably, ICOHP only integrates from –∞ to 0 because only the orbitals below the Fermi level are filled with electrons, which determines the bonding strength. While the orbitals above Fermi level are unoccupied ones, which have no effect on bonding strength. So, the physical meaning of ICOHP can be considered as the relative energy of effective bonding electrons number ($eN_{\text{bond electron}} - eN_{\text{anti-bond electron}}$, marked as, effective electron energy), which indicates that the number of bonding and anti-bonding orbital electrons is a crucial and important factor in determining adsorption strength. Unfortunately, ICOHP still ignores another key factor, the orbital energy levels of electrons [47], which may seriously limit the accuracy of ICOHP in quantitatively describing adsorption intensity.

### 3.3. Bonding and anti-bonding orbitals stable electron intensity difference (BASED) theory

Inspired by above analysis, we proposed the bonding and anti-bonding orbitals stable electron intensity difference (BASED) theory by combining D-band center, COHP and MO theory to serve as a general descriptor for quantitatively describing adsorption intensity, given by

$$BASED = \int_{-\infty}^{0} \varepsilon \times \rho_{\text{COHP}}(\varepsilon)d\varepsilon \quad (5)$$

This is a very ingenious equation. To understand its physical meaning, the following deduction is given by

$$BASED = \int_{-\infty}^{0} \varepsilon \times \rho_{\text{COHP-Bond}}(\varepsilon)d\varepsilon + \int_{-\infty}^{0} \varepsilon \times \rho_{\text{COHP-AntiBond}}(\varepsilon)d\varepsilon$$
$$= \frac{\int_{-\infty}^{0} \varepsilon \times \rho_{\text{COHP-Bond}}(\varepsilon)d\varepsilon}{\int_{-\infty}^{0} \rho_{\text{COHP-Bond}}(\varepsilon)d\varepsilon} \times \int_{-\infty}^{0} \rho_{\text{COHP-Bond}}(\varepsilon)d\varepsilon -$$
$$\frac{\int_{-\infty}^{0} \varepsilon \times \rho_{\text{COHP-AntiBond}}(\varepsilon)d\varepsilon}{\int_{-\infty}^{0} \rho_{\text{COHP-AntiBond}}(\varepsilon)d\varepsilon} \times \int_{-\infty}^{0} -\rho_{\text{COHP-AntiBond}}(\varepsilon)d\varepsilon$$
$$= \varepsilon_{\text{C-Bond}} \times \alpha eN_{\text{Bond electron}} - \varepsilon_{\text{C-Antibond}} \times \alpha eN_{\text{Antibond electron}} \quad (6)$$

where $eN_{\text{Bond electron}}$ and $eN_{\text{Antibond electron}}$ represent the energy of electrons for bonding orbitals and anti-bonding orbitals. $\rho_{\text{COHP-Bond}}(\varepsilon)$ and $\rho_{\text{COHP-Anti-Bond}}(\varepsilon)$ represent COHP proportions of bonding and anti-bonding orbitals; $\varepsilon_{\text{C-Bond}}$ and $\varepsilon_{\text{C-AntiBond}}$ represent the energy level centers of the bonding and anti-bonding orbitals, respectively, which was similar with the D-band center. We consider the product of orbital energy level of electrons and effective electrons energy as the intensity of stable electron (which is $\varepsilon_C \times \alpha eN_{\text{electron}}$), where the negative values represent stable state (electrons filling in bonding orbitals), and the positive values represent unstable state (electrons filling in anti-bonding orbitals). According to MO theory, molecular orbitals are split into bonding and anti-bonding orbitals. The electrons are preferring to fill into the bonding orbitals which are usually at the low energy level and make the bond more stable, while the electrons filled into anti-bonding orbitals are usually at the higher energy level, which weakens the stability of bond. So, it is obvious that BASED represents the difference between the products of electrons energy and their corresponding orbital energy level of electrons ($\varepsilon_C \times \alpha eN_{\text{electron}}$) in bonding orbitals and anti-bonding orbitals (Fig. 2(a)), and the BASED represents the stable intensity of orbitals electrons. Actually, the unit of BASED is eV², because BASED is a relevant term of $\varepsilon^2$. So, the BASED may be related to second-order moment $M_{2,i}^{\alpha}$ proposed by Prof. Xin [63] and $\Delta E_{d\text{-hyb}}$ proposed by Prof. Nørskov [23,64].

The difference between BASED and ICOHP is that ICOHP only considers the effective electrons energy, while BASED considers both the effective electrons energy and the orbital energy level of electrons. Fig. 2 was used to clarify the reason for the relatively low accuracy of ICOHP. Figs. 2(b) and 2(c) show two cases of bonding states, and they have the same effective electrons energy in both bonding and anti-bonding orbitals (the same area of COHP peak), but the anti-bonding orbitals are at lower energy levels in Fig. 2(b), while they are at higher energy levels in Fig. 2(c). Since ICOHP only considers the effective electrons energy, it predicts that the bond strengths of the two bonding states are the same. Obviously, ICOHP seriously ignores the fact of anti-bond orbital energy level shifting towards the higher energy level, which would make the bond more stable, i.e., the bonding strength in Fig. 2(b) should be significantly weaker than that in Fig. 2(c). Similarly, if the bonding orbital shifts towards the lower energy level, it will also increase the bonding strength. Therefore, the absence of orbital electron energy level is essential origin of relatively low accuracy of ICOHP. On the contrary, when the proportion of bonding orbitals and anti-bonding orbitals is fixed, we believe that the larger distance between bonding orbitals and anti-bonding orbitals would represent the stronger bond strength, which can be predicted by the BASED theory (Fig. 2(c)). In particular, Fig. 2(d) shows a special case, where all the anti-bonding orbitals are in the unoccupied orbital region. In this case, we set the center of the anti-bonding orbitals ($\varepsilon_{\text{C-AntiBond}}$) to 0. For the calculation convenience of investigators, we also provided a code here for calculating BASED, which needs the Python 3.x environment (BASED v1.0 program code) (see Supporting Files-BASED v1.0.py).

### 3.4. Verification and comparison of BASED

To verify the BASED theory, we conducted extensive calculations of adsorption energy for various adsorption configurations. Fig. 3 shows the simplified adsorption models which include ten types of single atom catalysts (SACs, including $ScN_4$, $TiN_4$, $VN_4$, $CrN_4$, $MnN_4$, $FeN_4$, $CoN_4$, $NiN_4$, $CuN_4$, $ZnN_4$, Fig. 3(a)) and Pt\Ni\Ag\Cu bulk models (Fig. 3(b)). The SACs models were used to systematically explore the atomic interaction due

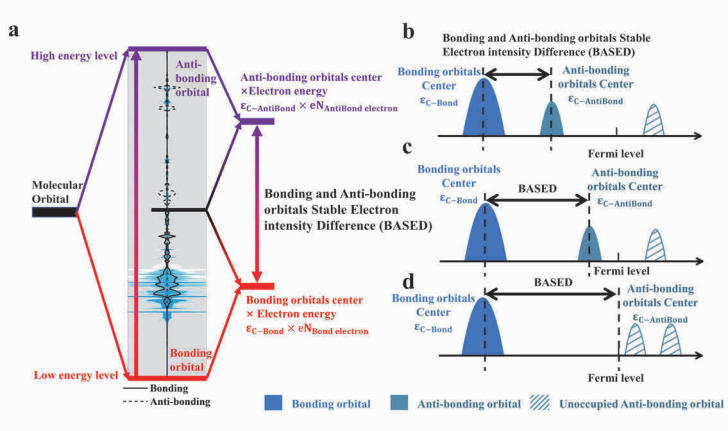


**Fig. 2.** Illustrations of BASED theory. (a) Schematic diagram of molecular orbital conversion to BASED. (b–d) Schematic diagram of three different bonding and anti-bonding orbitals, where the anti-bonding orbitals gradually right shift until they become unoccupied orbitals.

to its simple adsorption method, while the bulk models were used to validate our theory of atomic interaction through various adsorption methods. In addition, we additionally calculated the H*, O* and OH* adsorption data of all models to verify our understanding and explanation of the D-band center theory. We used about 180 SAC models which have different distances between active centers and H*, O* and OH* adsorbents, respectively (Fig. S1), to explore the influence of distance on atomic interactions.

The calculation result clearly supports our viewpoint for anti-D-band center phenomenon. Figs. 4(a)–(c) clearly show the relationship between the adsorption energy of H*, O*, OH* and D-band center, which exhibits a V-shaped trend. This means that the adsorption capability of the active site increases first and then decreases as the value of the D-band center ($\varepsilon_d$) increases. According to the $\varepsilon_d$ data which are displayed in Fig. S2 and Table S1, as the number of valence electrons in TM increases, the $\varepsilon_d$ exhibits a gradual left-shift from $ScN_4$ to $ZnN_4$ (from 2.828 to −5.967 eV, Fig. 4(d)). Fig. S2 also presented projected DOS information of detailed five types d orbits in 3*d* TM SACs. It is noted that $\varepsilon_d$ of $ScN_4$, $TiN_4$, $VN_4$, and $CrN_4$ is the positive value, which usually leads to bonding orbitals near the Fermi level (Figs. S3–S5), and the proportion of bonding orbitals would gradually increase with the decreased value of $\varepsilon_d$, resulting in the anti-D-band center phenomenon (Figs. 4(a)–(c) right leg). While $\varepsilon_d$ of $MnN_4$ ~ $ZnN_4$, and Pt\Ni\Ag\Cu bulk are negative values, which could lead to anti-bonding orbitals near the Fermi level and the proportion of anti-bonding orbitals would gradually increase when the value of $\varepsilon_d$ becomes more negative, and they can be explained by the D-band center theory (Figs. 4(a)–(c), left leg).

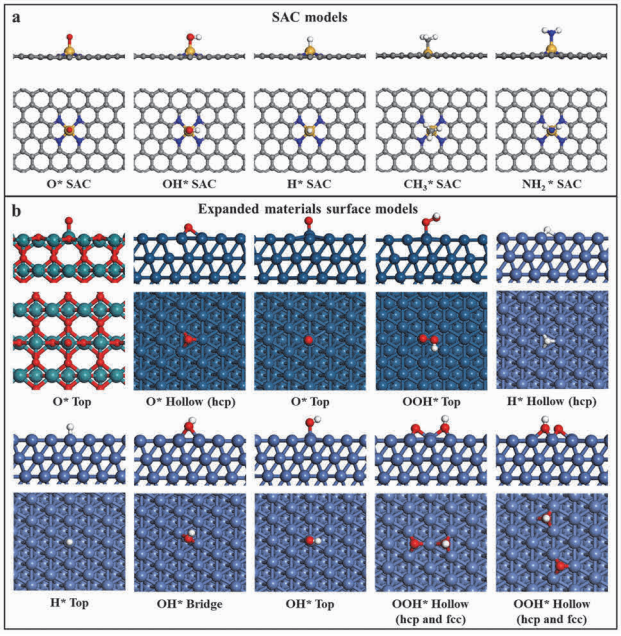


**Fig. 3.** Adsorption illustrations of different surface models. (a) The O*, OH*, H*, $CH_3$* and $NH_2$* adsorption models of SAC, including all kinds of 3d transition metal SACs. (b) The O*, OH*, OOH* and H* adsorption models of expanded material surface models (Bulk models) after adsorption, including $RuO_2$ (001), Pt (111), Ni (111), Ag (111), and Cu (111) bulk models.

To verify the accuracy of BASED in quantifying adsorption intensity, we also used adsorption energy to comprehensively compare BASED with ICOHP, which includes all these data from all kinds of adsorption forms in above Figs. 3(a) and (b). Since the unit of BASED is $eV^2$, thus we adopted a parameter *Q* (an abbreviation for Quantum) whose unit is eV (Eq. (7)) as a general descriptor to predict the adsorption energy of activity center.

$$Q = \sqrt{BASED} = \sqrt{\int_{-\infty}^{0} \rho_{COHP}(\varepsilon)\varepsilon d\varepsilon} \quad (7)$$

Obviously, Fig. 4(f) shows a well linear relationship between *Q* and adsorption energy, where the correlation factor $R^2$ for adsorption energy reaches 0.95 (*Q*, Fig. 4(f)), where a larger *Q* value means a stronger adsorption energy. On the contrary, for ICOHP (see Tables S2–S13 for the detailed data), the correlation factor $R^2$ for adsorption energy is only 0.75 (ICOHP, Fig. 4(e)), due to the lack of orbital electron energy level information in ICOHP. Moreover, the COHP-DOS diagrams of the adsorbent and surface (Figs. S6–S26) also show that as the adsorbents (H*, O* and OH*) gradually stay away from the surface ($CrN_4$, $MnN_4$, $FeN_4$, $CoN_4$, $NiN_4$, $CuN_4$, $ZnN_4$,), the distance between the bonding and anti-bonding orbitals gradually approaches (also meaning that adsorption capability and bond

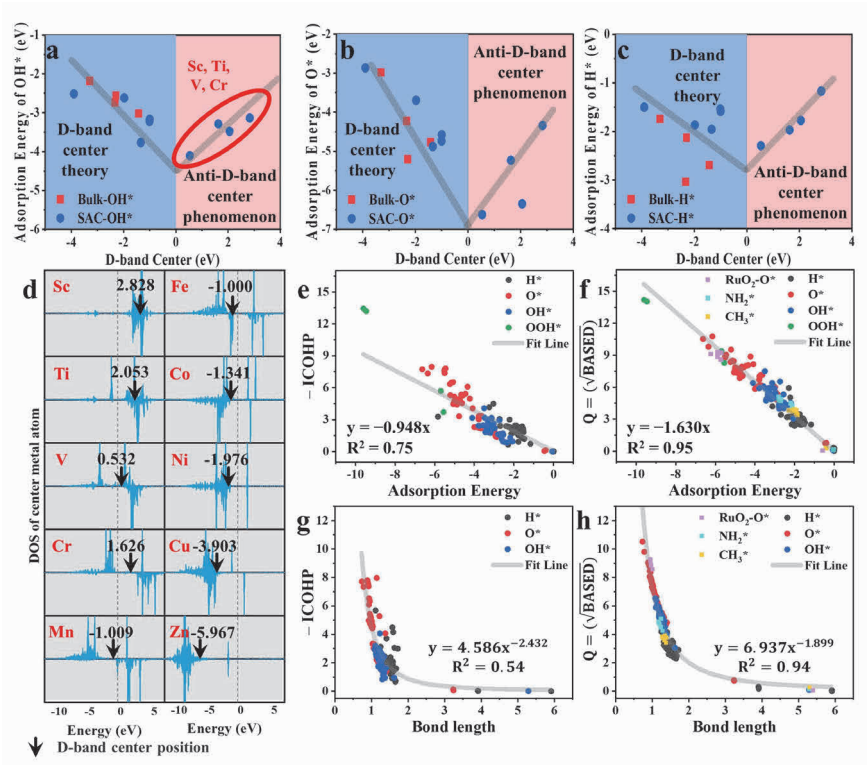


**Fig. 4.** Theoretical calculation results from different methods. The relationship between adsorption energy of intermediates and $\varepsilon_d$, OH* (a), O* (b) and H* (c). (d) The red circle represents four types of SACs with anti-D-band center phenomenon. (e) Projected DOS (PDOS) diagram of all 3d metal SACs slab. (f) The relationship between −ICOHP and adsorption energy. The larger the −ICOHP, the stronger the adsorption capability. The relationship between $Q$ and adsorption energy. The larger the $Q$, the stronger the adsorption capability. (g) The relationship between −ICOHP and bond length. (h) The relationship between $Q$ and bond length.

strength weaken). Until the distance is far enough, both the bonding and anti-bonding orbitals disappear. This phenomenon provides a solid evidence to prove the physical insight of BASED, i.e., the distance between the bond orbital and the anti-bond orbital is also a key factor of adsorption strength.

To make the BASED theory more universal, we conducted a detailed study on the relationship between $Q$ and bond length, and also made a comparison with ICOHP. By correcting atomic radius (Fig. S27), Figs. 4(h) and (g) show that the correlation $R^2$ of BASED with bond length can reach 0.94, while it is 0.54 for ICOHP. Such a high correlation $R^2$ indicates that BASED can serve as the general descriptor for the next generation simulation software, which can be used in chemistry, biology, and semiconductors and other field. It should be pointed out that accuracy of BASED in predicting adsorption energy may be affected by the accuracy of DOS and COHP (about 3%–5%). In short, the BASED provides a more accurate method for revealing adsorption phenomena from the viewpoint of electronic structure.

Moreover, the metal oxide systems are also the semiconductor systems, and the active sites are also the exposed metal atoms on the surface. Thus, the adsorption behavior of metal oxide systems should be similar to that of SACs systems [65,66]. When the BASED theory is applicable to the SACs, it should be also applicable to the metal oxide system. Similarly, when the BASED theory is applicable to the SACs adsorbing H*, O*, OH*, and OOH*, the BASED theory should also be applicable to the SAC adsorbing other molecules such as $NH_2$* and $CH_3$*. To confirm this conclusion, we used these data from $RuO_2$-O* and $FeN_4$-$NH_2$*/$CH_3$* as validation sets (Figs. 4(f) and (h), Tables S26–S29). All the results indicate that the BASED theory is applicable to newly-calculated data.

### 3.5. *Spin transition state phenomenon*

Interestingly, when the BASED was used to investigate the adsorption center and the spin flip (Fig. S1, Figs. 5(a)–(c)), we accidentally discovered that the magnetic moment of the active center atom is usually not a fixed value. In the process of adsorbent approaching adsorption center, the active center atom usually has a high spin transition state (Tables S14–S25). This may be due to the bands of two different spins are affected differently, making the up-spin bands relatively lower in energy, which causes the spin polarization in the periodic systems. And this transition state will disappear and become a low spin state when the distance of adsorbent and the surface is small enough. As shown in Figs. 5(d)–(f) and Fig. S28, when the distance between the adsorbent and the surface is about 4–6 Å, the active center is usually at a low magnetic moment, for example, the magnetic moment of $FeN_4$ slab is 2 μB (Fig. 5(d)), $CoN_4$ slab is 1 μB (Fig. 5(e)) and $NiN_4$ slab is 0 μB (Fig. 5(f)). However, as the distance is about 2.5 Å, the magnetic moment of the active center suddenly increases, and magnetic moment of $FeN_4$ increases to 4 μB, and they are 3 μB for $CoN_4$ and 2 μB

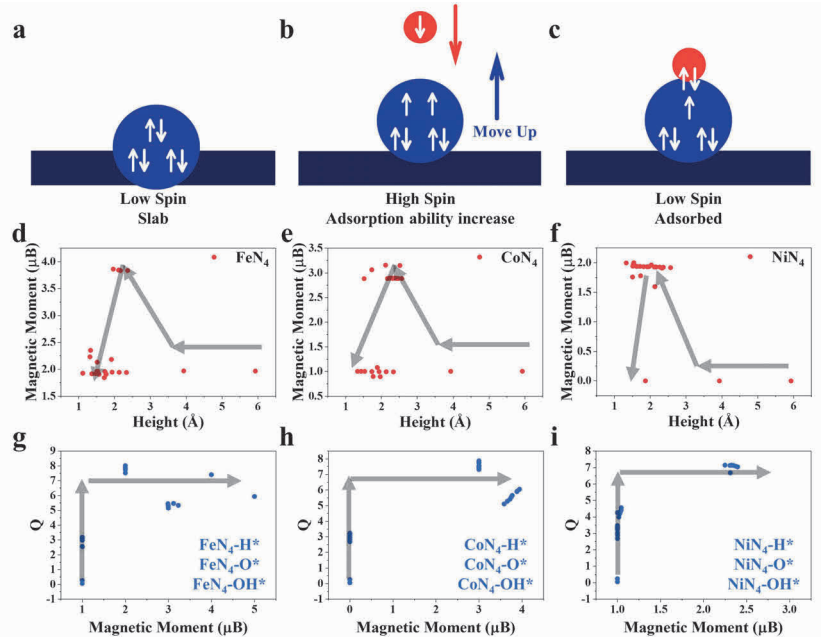


**Fig. 5.** Illustrations of STS phenomenon. (a) Schematic diagram of active center atoms in low spin state. (b) Schematic diagram of active center atoms in high spin state. (c) Schematic diagram of active center atoms completing adsorption process. The relationship between magnetic moment of active center atoms and the distance between the adsorbent (H*, O* and OH*) and slab, based on $FeN_4$ (d), $CoN_4$ (e), $NiN_4$ (f), where the gray arrow represents the trend of magnetic moment variation with height. The relationship between magnetic moment of active center atoms and *Q*, based on $FeN_4$ (g), $CoN_4$ (h), $NiN_4$ (i). High value of *Q* represents strong adsorption capability of the active center atom. The gray arrow represents the trend of the adsorption capability indicator *Q* with respect to magnetic moment.

for $NiN_4$. When the distance becomes smaller (say, less than 2 Å), the magnetic moment of the active center atom returns to its original low spin state. This phenomenon is similar to the transition state process, and Fig. S29 shows that the relative energy of the surface significantly increases at 2.5 Å as the adsorbent approaches the surface, and then drops back to the stable low spin state, which means that the high spin state is an unstable transition state. During this process, there is an energy barrier of 0.3–2 eV, which is relatively weak for $CrN_4$, $MnN_4$, and $FeN_4$ (usually less than 0.8 eV), but higher for $CoN_4$, $NiN_4$, $CuN_4$, and $ZnN_4$ (1.5–2 eV). This may be the intrinsic reason why $FeN_4$ species always have good electrocatalytic activity. The phenomenon exists in almost all the processes of active centers adsorbing adsorbents, and we marked it as Spin Transition State (STS).

In order to reveal the origin of STS, we quantitatively analyzed the adsorption capability of active centers by using the BASED theory. Figs. 5(g)–(i) and Fig. S30 show that the adsorption capability of active centers is usually weak or sometimes almost zero at low spin, while at high spin, their adsorption capability is greatly enhanced, with an increase of more than 3 times. For example, the adsorption capability in low spin of $FeN_4$ slab is 0–2.5 (Fig. 5(g)), $CoN_4$ slab is 0–3 (Fig. 5(h)) and $NiN_4$ slab is 0–3 (Fig. 5(i)) which were calculated by BASED. While the adsorption capability in high spin of $FeN_4$ slab is 5.5–8, $CoN_4$ slab is 5–8 and $NiN_4$ slab is 6.5–7. So, the high adsorption strength of high spin states may be due to the fact that high magnetic moments result in a large energy level difference between bonding orbitals and anti-bonding orbitals. Based on the above analysis, we believe that active center atoms with high spin states often have a high adsorption capability but a low stability, while active center atoms with low spin states often have a high stability but a low adsorption capability. This phenomenon indicates that the active center is in the low spin state initially (Fig. 5(a)) and then the active center is activated by the adsorbed molecules to the high spin state (Fig. 5(b)), which improves its adsorption capability. The appearance of high spin state may be attributed to the fact that the active center atoms tends to increase its coordination number to offset the axial strain effect caused by the adsorbent. After the adsorption process is completed, the system will back to a low spin state (such as $FeN_4$, $CoN_4$, $NiN_4$, Figs. 5(d)–(f)) because the high spin state is usually unstable. However, in some cases, if the high spin is a relatively stable state, it may still remain in the high spin state (such as $MnN_4$, Fig. S28), which is the reason why both high spin and low spin states exist at 1–2.5 Å. It is noted that an excessive high spin state may not lead to a stronger adsorption capability due to instability. For example, $CrN_4$, $MnN_4$, and $ZnN_4$ (Fig. S30) initially have strong adsorption capability at relatively high spin states, but when they reach higher spin states, their adsorption capability would suddenly decrease due to their excessive instability. Actually, by the BASED theory, we discovered that the active center atoms usually exist a relatively unstable STS with a high spin magnetic moment in the adsorption process, which is favorable for adsorbing intermediates.

## 4. Conclusions

In summary, we have proposed the BASED theory as a gen-

eral descriptor to quantitatively depict adsorption capability of active sites, include SACs, bulk and other systems which have different adsorption methods. Simultaneously, we also explained the puzzles why the anti-D-band center phenomenon exists. Compared with the existing ICOHP, the BASED theory exhibits very high accuracy for predicting adsorption capability ($R^2$ = 0.95). Therefore, BASED can serve as the general descriptor for the next generation simulation software, which can be used in chemistry, biology, and semiconductors and other fields. The BASED v1.0 program code was also provided for use of readerships.

By using BASED, we found the existence of spin transition state (STS) in surface adsorption, i.e. the active center atom usually has a high spin transition state at about 2.5 Å distance between active site and adsorbent in the adsorption process, which has a high adsorption capability but a low stability. During this process, the adsorption capability of high spin states is usually three times higher than that of low spin states predicted by BASED. After the adsorption process is completed, the active center atom will return into a more stable low spin state or stay in a relatively stable high spin state, which depends on the relative energy. This novel STS phenomenon provides a new physical insight into understanding surface catalysis processes and can greatly promote the development of surface chemistry.

## Electronic supporting information

The BASED v1.0 code was provided, and Supporting information is available in the online version of this article.

## Competing Interest

The authors declare no competing financial interest

## References


[1] P. Li, Y. L. Jiang, Y. C. Hu, Y. N. Men, Y. W. Liu, W. B. Cai, S. L. Chen, *Nat. Catal.*, **2022**, 5, 900–911.

[2] X. Li, Z. Huang, C. E. Shuck, G. Liang, Y. Gogotsi, C. Zhi, *Nat. Rev. Chem.*, **2022**, 6, 389–404.

[3] Z.-Y. Wu, F.-Y. Chen, B. Li, S.-W. Yu, Y. Z. Finfrock, D. M. Meira, Q.-Q. Yan, P. Zhu, M.-X. Chen, T.-W. Song, Z. Yin, H.-W. Liang, S. Zhang, G. Wang, H. Wang, *Nat. Mater.*, **2023**, 22, 100–108.

[4] Y. Luo, Z. Zhang, M. Chhowalla, B. Liu, *Adv. Mater.*, **2022**, 34, 2108133.

[5] Z. Niu, Z. Lu, Z. L. Qiao, S. T. Wang, X. Cao, X. D. Chen, J. Yun, L. R. Zheng, D. P. Cao, *Adv. Mater.*, **2024**, 36, 2310690.

[6] T. Pu, W. Zhang, M. Zhu, *Angew. Chem. Int. Ed.*, **2023**, 62, e202212278.

[7] Y. B. Qi, Y. Zhang, L. Yang, Y. H. Zhao, Y. H. Zhu, H. L. Jiang, C. Z. Li, *Nat. Commun.*, **2022**, 13, 4602.

[8] J. X. Guo, Y. Zheng, Z. P. Hu, C. Y. Zheng, J. Mao, K. Du, M. Jaroniec, S. Z. Qiao, T. Ling, *Nat. Energy*, **2023**, 8, 264–272.

[9] P. Sun, Z. Qiao, X. Dong, R. Jiang, Z. T. Hu, J. Yun, D. Cao, *J. Am. Chem. Soc.*, **2024**, 146, 15515–15524.

[10] X. Ding, R. Jiang, J. Wu, M. Xing, Z.L. Qiao, X. Zeng, S. T. Wang, D. P. Cao, *Adv. Funct. Mater.*, **2023**, 33, 2306786.

[11] A. Gross, S. Sakong, *Chem. Rev.*, **2022**, 122, 10746–10776.

[12] X. X. Wei, B. Zhang, B. Wu, Y. J. Wang, X. H. Tian, L. X. Yang, E. E. Oguzie, X. L. Ma, *Nat. Commun.*, **2022**, 13, 726.

[13] B. Zhang, Q. Zhu, C. Xu, C. Li, Y. Ma, Z. Ma, S. Liu, R. Shao, Y. Xu, B. Jiang, L. Gao, X. Pang, Y. He, G. Chen, L. Qiao, *Nat. Commun.*, **2022**, 13, 3858.

[14] X. Kang, F. Yang, Z. Zhang, H. Liu, S. Ge, S. Hu, S. Li, Y. Luo, Q. Yu, Z. Liu, Q. Wang, W. Ren, C. Sun, H.-M. Cheng, B. Liu, *Nat. Commun.*, **2023**, 14, 3607.

[15] E. Perez-Botella, S. Valencia, F. Rey, *Chem. Rev.*, **2022**, 122, 17647–17695.

[16] C. Wu, X. Wang, Y. Tang, H. Zhong, X. Zhang, A. Zou, J. Zhu, C. Diao, S. Xi, J. Xue, J. Wu, *Angew. Chem. Int. Ed.*, **2023**, 62, e202218599.

[17] H. X. Xu, D. Cheng, D. P. Cao, X. C. Zeng, *Nat. Catal.*, **2024**, 7, 207–218.

[18] H. X. Xu, D. Cheng, D. P. Cao, X. C. Zeng, *Nat. Catal.*, **2018**, 1, 339–348.

[19] B. Hammer, J. K. Nørskov, *Surf. Sci.*, **1995**, 343, 211–220.

[20] B. Hammer, J. K. Norskov, *Nature*, **1995**, 376, 238–240.

[21] B. Hammer, J. K. Nørskov, *Adv. Catal.*, **2000**, 45, 71–129.

[22] J. K. Norskov, F. Abild-Pedersen, F. Studt, T. Bligaard, *Proc. Natl. Acad. Sci. U. S. A.*, **2011**, 108, 937–943.

[23] J. K. Nørskov, F. Studt, F. Abild-Pedersen, T. Bligaard, in: *Funda-*


## Graphical Abstract

*Chin. J. Catal.*, 2024, 64: 44–53 doi: 10.1016/S1872-2067(24)60100-2

**Why the abnormal phenomena of D-band center theory exist? A new BASED theory for surface catalysis and chemistry**

Zelong Qiao, Run Jiang, Jimmy Yun, Dapeng Cao *
*Beijing University of Chemical Technology, China;*
*Qingdao International Academician Park Research Institute, China;*
*The University of New South Wales, Australia*

This work proposes a bonding and anti-bonding orbitals stable electron intensity difference (BASED) theory to reveal the origin of abnormal phenomena of D-band center theory. The high-precision descriptor *Q* is obtained to quantitatively predict adsorption energy and bond length.

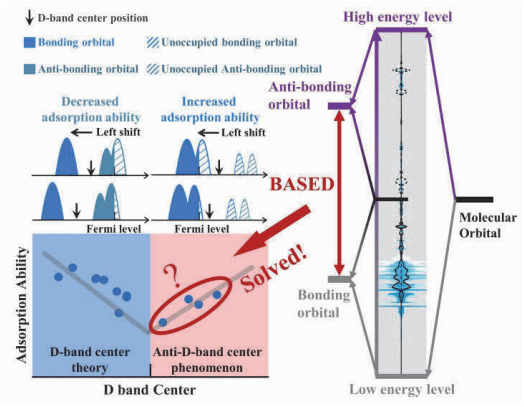

*mental Concepts in Heterogeneous Catalysis*, John Wiley & Sons, Inc., **2014**, 114–137.
[24] Z. Hou, C. Cui, Y. Li, Y. Gao, D. Zhu, Y. Gu, G. Pan, Y. Zhu, T. Zhang, *Adv. Mater*., **2023**, 35, 2209876.
[25] Z. Y. Xiao, P. P. Sun, Z. L. Qiao, K. W. Qiao, H. X. Xu, S. T. Wang, D. P. Cao, *Chem. Eng. J*., **2022**, 446, 137112.
[26] S. Q. Huang, Z. L. Qiao, P. P. Sun, K. W. Qiao, K. Pei, L. Yang, H. X. Xu, S. T. Wang, Y. Huang, Y. S. Yan, D. P. Cao, *Appl. Catal. B*, **2022**, 317, 121770.
[27] T. H. Yu, T. Hofmann, Y. Sha, B. V. Merinov, D. J. Myers, C. Heske, W. A. Goddard III, *J. Phys. Chem. C*, **2013**, 117, 26598–26607.
[28] A. Vojvodic, J. K. Norskov, F. Abild-Pedersen, *Top. Catal.*, **2014**, 57, 25–32.
[29] S. Saini, J. Halldin Stenlid, F. Abild-Pedersen, *npj Comput. Mater*., **2022**, 8, 163.
[30] D. Wu, K. Kusada, Y. Nanba, M. Koyama, T. Yamamoto, T. Toriyama, S. Matsumura, O. Seo, I. Gueye, J. Kim, L. S. R. Kumara, O. Sakata, S. Kawaguchi, Y. Kubota, H. Kitagawa, *J. Am. Chem. Soc*., **2022**, 144, 3365–3369.
[31] Y. Nanba, M. Koyama, *J. Phys. Chem. C*, **2019**, 123, 28114–28122.
[32] M. Li, Z. Li, X. Yu, Y. Wu, C. Mo, M. Luo, L. Li, S. Zhou, Q. Liu, N. Wang, K. L. Yeung, S. Chen, *Chem. Eng. J*., **2022**, 431, 133339.
[33] Y. Wang, W. Cheng, P. Yuan, G. Yang, S. Mu, J. Liang, H. Xia, K. Guo, M. Liu, S. Zhao, G. Qu, B.-A. Lu, Y. Hu, J. Hu, J.-N. Zhang, *Adv. Sci.*, **2021**, 8, 2102915.
[34] Z. Duan, G. Henkelman, *ACS Catal.*, **2020**, 10, 12148–12155.
[35] L. Zhao, J. H. Yan, H. J. Huang, X. Du, H. Chen, X. He, W. X. Li, W. Fang, D. H. Wang, X. H. Zeng, J. C. Dong, Y. Q. Liu, *Adv. Funct. Mater*., **2023**, 34, 2310902.
[36] D. M. Janas, A. Droghetti, S. Ponzoni, I. Cojocariu, M. Jugovac, V. Feyer, M. M. Radonjic, I. Rungger, L. Chioncel, G. Zamborlini, M. Cinchetti, *Adv. Mater*., **2023**, 35, 2205698.
[37] K. Liu, J. Fu, Y. Lin, T. Luo, G. Ni, H. Li, Z. Lin, M. Liu, *Nat. Commun*., **2022**, 13, 2075.
[38] R. Jiang, Z. L. Qiao, H. X. Xu, D. P. Cao, *Chin. J. Catal.*, **2023**, 48, 224–234.
[39] R. Jiang, Z. Qiao, H. Xu, D. Cao, *Nanoscale*, **2023**, 15, 16775–16783.
[40] H. Liu, J. Gao, X. Xu, Q. Jia, L. Yang, S. T. Wang, D. P. Cao, *Chem. Eng. J*., **2022**, 448, 137706.
[41] Z. X. Song, X. Chi, S. Dong, B. Meng, X. J. Yu, X. L. Liu, Y. Zhou, J. Wang, *Angew. Chem. Int. Ed*., **2024**, 63, e202317267.
[42] X. F. Yang, A. Wang, B. Qiao, J. Li, J. Liu, T. Zhang, *Acc. Chem. Res*, **2013**, 46, 1740–1748.
[43] Z. Y. Jin, P. P. Li, Y. Meng, Z. W. Fang, D. Xiao, G. H. Yu, *Nat. Catal.*, **2021**, 4, 615–622.
[44] L. Yang, D. Cheng, H. X. Xu, X. Zeng, X. Wan, J. Shui, Z. Xiang, D. P. Cao, *Proc. Natl. Acad. Sci. U. S. A.*, **2018**, 115, 6626–6631.
[45] L. Yang, L. Shi, D. Wang, Y. Lv, D. P. Cao, *Nano Energy*, **2018**, 50, 691–698.
[46] J. Zhang, X. Xu, L. Yang, D. Cheng, D. P. Cao, *Small Methods*, **2019**, 3, 1900653.
[47] Z. Qiao, R. Jiang, H. Xu, D. Cao, X. C. Zeng, *Angew. Chem. Int. Ed*., **2024**, 63, e202407812.
[48] G. Kresse, J. Furthmüller, *Comput. Mater. Sci*, **1996**, 6, 15–50.
[49] K. Mathew, R. Sundararaman, K. Letchworth-Weaver, T.A. Arias, R.G. Hennig, *J. Chem. Phys.*, **2014**, 140, 084106.
[50] R. Nelson, C. Ertural, J. George, V.L. Deringer, G. Hautier, R. Dronskowski, *J. Comput. Chem.*, **2020**, 41, 1931–1940.
[51] V. L. Deringer, A.L. Tchougreeff, R. Dronskowski, *J. Phys. Chem. A*, **2011**, 115, 5461–5466.
[52] P. Sun, Z. Qiao, S. Wang, D. Li, X. Liu, Q. Zhang, L. Zheng, Z. Zhuang, D. Cao, *Angew. Chem. Int. Ed*., **2023**, 62, e202216041.
[53] J. Hwang, R. R. Rao, L. Giordano, Y. Katayama, Y. Yu, Y. Shao-Horn, *Science*, **2017**, 358, 751–756.
[54] X. J. Xin, C. S. Guo, R. Pang, X. Q. Shi, Y. Zhao, *Appl. Surf. Sci.*, **2021**, 570, 151126.
[55] Y. Sun, S. Sun, H. Yang, S. Xi, J. Gracia, Z. J. Xu, *Adv. Mater.*, **2020**, 32, 2003297.
[56] X. Q. Wei, S. J. Song, W. W. Cai, X. Luo, L. Jiao, Q. Fang, X. S. Wang, N. N. Wu, Z. Luo, H. J. Wang, Z. H. Zhu, J. Li, L. R. Zheng, W. L. Gu, W. Y. Song, S. J. Guo, C. Z. Zhu, *Chem*, **2023**, 9, 181–197.
[57] C. Chen, W. Chen, Q. Liu, Y. Liu, G. Xiao, C. Chen, F. Li, J. Zhou, *ACS Appl. Nano Mater.*, **2022**, 5 12646–12655.
[58] G. Feng, M. Gao, L. Wang, J. Chen, M. Hou, Q. Wan, Y. Lin, G. Xu, X. Qi, S. Chen, *Nat. Commun.*, **2022**, 13, 2652.
[59] G. Wu, X. Han, J. Cai, P. Yin, P. Cui, X. Zheng, H. Li, C. Chen, G. Wang, X. Hong, *Nat. Commun.*, **2022**, 13, 4200.
[60] Z. Chen, J. Wang, M. Hao, Y. Xie, X. Liu, H. Yang, G. I. N. Waterhouse, X. Wang, S. Ma, *Nat. Commun.*, **2023**, 14, 1106.
[61] S. Maintz, V. L. Deringer, A. L. Tchougreeff, R. Dronskowski, *J. Comput. Chem*., **2016**, 37, 1030–1035.
[62] S. Maintz, V. L. Deringer, A. L. Tchougreeff, R. Dronskowski, *J. Comput. Chem*., **2013**, 34, 2557–2567.
[63] X. Ma, H. Xin, *Phys. Rev. Lett.*, **2017**, 118, 036101.
[64] A. Ruban, B. Hammer, P. Stoltze, H. L. Skriver, J. K. Nørskov, *J. Mol. Catal. A*, **1997**, 115, 421–429.
[65] R. Qi, B. Zhu, Z. Han, Y. Gao, *ACS Catal.*, **2022**, 12, 8269–8278.
[66] A. Allangawi, N. Kosar, K. Ayub, M. A. Gilani, N. H. B. Zainal Arfan, M. H. S. A. Hamid, M. Imran, N. S. Sheikh, T. Mahmood, *ACS Omega*, **2023**, 8, 37820–37829.

# D带中心理论的反常现象缘何存在?一个用于表面化学的新理论——“BASED理论”

乔泽龙[a], 姜　润[a], Jimmy Yun [b,c], 曹达鹏[a,*]
[a]北京化工大学, 有机无机复合材料国家重点实验室, 北京100029, 中国
[b]青岛国际院士港研究院, 山东青岛266000, 中国
[c]新南威尔士大学化学工程学院, 新南威尔士州, 澳大利亚

**摘要**: 自D带中心理论提出以来, 因其易于理解、使用简便且相对准确, 已被广泛应用于表面化学的研究中. 然而, 在实际应用中, 其反常现象却时常出现, 这促使研究者们重新审视D带中心理论在表面催化与化学领域中应用的局限性. 随着材料科学及合成技术的飞速发展, 在小型金属粒子体系和半导体材料体系(特别是单原子体系), D带中心理论的局限性愈发凸显, 导致了许多与其预期不符的结论. 鉴于D带中心理论原本是基于较大金属粒子体系构建的, 因此, 深入探究D带中心

理论反常现象的根源, 并构建新的理论以解决这一问题具有重要意义.

本文通过分析D带中心理论的起源及其物理意义, 发现有两个原因导致其出现反常现象: 一是仅考虑了轨道能级位置而忽略了电子数所带来的影响; 二是只考虑了材料整体的电子性质, 忽略了表面上存在多种活性位点以及吸附方式的多样性. 此外, 对于已有的表征键强度的描述符——晶体轨道哈密顿布居(COHP)所衍生出来的ICOHP, 其仅考虑了电子数的影响, 而忽略了轨道能级位置的作用, 这也导致存在较大的误差. 因此, 我们认为同时考虑轨道能级位置与电子数才能更准确地表征键的强度. 由于成键轨道可以增强键的强度, 而反键轨道则会削弱, 所以成键轨道与反键轨道之间的差值应该是一个有效的用于预测吸附能强弱的描述符. 基于上述分析, 我们提出了一个成键和反键轨道稳定电子强度差(BASED)的新理论. 为了验证该理论的准确性, 构建了包括金属颗粒表面(Pt(111), Ni(111), Ag(111)和Cu(111))、单原子催化剂(SACs, 包括$ScN_4$~$ZnN_4$)和金属氧化物表面($RuO_2$(001))在内的多种模型体系, 并计算了这些模型体系对H*、O*、OH*、OOH*、$CH_3$*和$NH_2$*中间体的吸附行为. 结果表明, BASED理论在预测吸附能和键长方面展现出极高的准确性(相关系数$R^2$分别为0.95和0.94), 远超ICOHP及D带中心描述符. 为了方便研究者们使用BASED理论、并推动其在表面化学领域的发展, 我们开发了基于Python的BASED v1.0程序, 供学术界免费使用. 此外, 值得注意的是, 基于BASED理论, 观察到了吸附过程中的一个奇特现象——自旋过渡态(STS). 即在吸附过程中, 活性中心原子在特定距离(约2.5 Å)处会呈现出高自旋过渡态来提升其吸附能力, 但稳定性相对较低; 而在吸附过程结束后, 高自旋态有时会转化为更稳定的低自旋态(是否转化取决于高自旋态与低自旋态的相对能量). 自旋过渡态现象可以为理解表面催化机制提供新的视角, 有助于研究者更好的理解活性位的吸附行为.

总之, BASED理论为表面化学和催化领域提供了新的描述符, 使研究者可以通过电子结构更精确地分析表面化学中的吸附和反应行为. 此外, 自旋过渡态现象为理解表面催化过程提供了新的物理视角, 能有效促进研究者对表面催化与化学反应机制的理解.

**关键词**: 表面化学; 表面催化; D带中心理论; 成键轨道; 反键轨道

收稿日期: 2024-05-09. 接受日期: 2024-06-24. 上网时间: 2024-09-10.

*通讯联系人. 电子信箱: caodp@mail.buct.edu.cn (曹达鹏).

基金来源: 国家重点研发计划(2019YFA0210300); 国家自然科学基金(22372006).